ELSEVIER

Polymer 42 (2001) 981–990

polymer

www.elsevier.nl/locate/polymer

Relation of glass transition temperature to the hydrogen-bonding degree and energy in poly(*N*-vinyl pyrrolidone) blends with hydroxyl-containing plasticizers. Part 2. Effects of poly(ethylene glycol) chain length

M.M. Feldstein[a,*], S.A. Kuptsov[b], G.A. Shandryuk[a], N.A. Platé[a]

[a]*A.V. Topchiev Institute for Petrochemical Synthesis, Russian Academy of Sciences, 29 Leninsky prospekt, 117912, Moscow, Russia*
[b]*Department of Physics, Moscow State Pedagogical University, 1, Malaya Pirogovskaya, 119882, Moscow, Russia*

Received 17 February 2000; received in revised form 1 May 2000; accepted 12 June 2000

Abstract

A phenomenological approach has been developed to evaluate a variety of the characteristics of hydrogen bonding in poly(*N*-vinyl pyrrolidone) (PVP) miscible blends with short chain poly(ethylene glycol) (PEG), ranging in molecular weight from 200 to 1000 g mol^{-1}. The approach is based on the analysis of experimentally measured composition dependence of the negative deviations in glass transition temperature, T_g, from weight-average values predicted by the Fox equation. The PVP–PEG miscibility is a result of hydrogen bonding between carbonyl groups in PVP repeat units and both terminal hydroxyls of PEG short chains. Because PEG macromolecules bear reactive hydroxyl groups only at both chain ends, the PVP–PEG complex has a network supramolecular structure. Influence of blend composition and PEG molecular weight on the mechanism of hydrogen bonding, the structure and the stoichiometry of the PVP–PEG complex have been studied. The significance of this work is two-fold. First, the validity of the approach suggested for determining the stoichiometry, network density and the thermodynamics of hydrogen-bonded complex formation in PVP–PEG systems has been confirmed by the results of independent measurements. Second, the nonequimolar stoichiometry of the hydrogen-bonded complex has been explained taking into account the counterbalancing contributions of the entropic loss caused by PEG chain immobilization by hydrogen bonding to PVP repeat units through both PEG chain-end hydroxyls, and the entropic gain due to the increase of the mobility of PVP chain segments between neighbouring hydrogen-bonded PEG crosslinks in the PVP–PEG network.

Keywords: Poly(*N*-vinyl pyrrolidone)–poly(ethylene glycol) blends; Glass transition temperature; Quantification of hydrogen-bonding degree and energy

1. Introduction

Poly(*N*-vinyl pyrrolidone) (PVP) and poly(ethylene glycol) (PEG) contain only electron-donating groups in their repeat units. It is therefore no wonder that PVP has been shown to be immiscible with high molecular weight PEG [1]. At the same time, PVP is reported to be soluble in liquid PEG having a molecular weight of 400 g mol^{-1} [2] and this behaviour implies the contribution of proton-donating terminal hydroxyl groups of oligomeric PEG to the compatibility with PVP. Actually, PVP is immiscible with dimethyl ether of PEG-400, DMPEG, whose chain-end reactive protons are replaced by inert methylene groups [3]. As has been established by FTIR spectroscopy, the compatibility of PVP blends with PEG-400 is due to hydrogen bonding of PEG terminal hydroxyls to the carbonyls in PVP repeat units [3,4]. The nitrogen atom of PVP amide groups and the oxyethylene units in PEG chains are not involved in PVP–PEG hydrogen bonding [4].

The hydrogen-bonded PVP complex with PEG-400 demonstrates a nonequimolar stoichiometry [5–7] and physical properties, which are not typical for unblended polymers: rubber-like elasticity [4] and pressure-sensitive adhesion toward diverse substrates [8]. Because reactive OH groups are located at both ends of the PEG chains, PEG behaves as a hydrogen-bonding telechelic crosslinker and the PVP–PEG complex reveals a supramolecular network structure [4]. Due to an appreciable length and flexibility of hydrogen-bonded PEG, the PVP–PEG network exhibits a unique combination of a high cohesive strength inherent in cured rubbers with an enhanced free volume, which ensure a liquid-like molecular mobility of polymer segments in the complex.

Molecular interactions in miscible polymer blends influence the composition dependence of glass transition

* Corresponding author. Fax: +7-095-230-2224.
E-mail address: mfeld@ips.ac.ru (M.M. Feldstein).

0032-3861/01/$ - see front matter
PII: S0032-3861(00)00439-0

temperature, T_g. The contributions of enhanced free volume, strong favourable interaction and mutual orientation of PVP and PEG chains are embedded in the compositional dependence of the T_g in PVP–PEG blends [4,7,9,10]. Meanwhile, it is also highly desirable to have a simple scheme for correlating the T_g with the measurements of intermolecular interactions, such as bonding degree and energy. In the first paper of this series [6] we have attempted to express in explicit form the negative T_g deviations from the weight-average magnitudes described by the Fox equation [11] through the number of polymer–plasticizer hydrogen bonds. In miscible PVP blends, with the plasticizers bearing two or three hydroxyl groups in their molecules (PEG and glycerol, respectively), the Fox equation fails to account for the large negative T_g deviations, because the original form of this equation relates T_g to the weight fractions of blend components, whereas that is the function of appropriate reactive groups' fractions (hydroxyls of the plasticizers and carbonyls in PVP repeat units). The fitting parameter, w_{pl}^*, introduced into the Fox equation, provides a direct measure of the negative T_g deviations and has a well-defined physical meaning, characterizing the weight fraction of plasticizer molecules that form two or more hydrogen bonds with the polymer. In this way, w_{pl}^* connects the measured T_g with a variety of important quantities, describing the dynamics of polymer–plasticizer hydrogen bonding. The w_{pl}^* parameter can be easily determined from the known T_g and requires no complementary data for evaluating the dynamics and stoichiometry of polymer–plasticizer hydrogen bonding and crosslinking.

This paper generalizes our approach proposed in the first paper of this series [6] for the case of PVP blends with PEG having different chain lengths. The characteristics of the PVP–PEG hydrogen-bonded network are analysed using the T_g–composition dependence. The equilibrium constant and the energy of PVP–PEG association into a crosslinked supramolecular structure of a hydrogen-bonded stoichiometric complex are calculated as well. The computed results are compared with the data of independent measurements in order to demonstrate the validity of the method and to gain a further insight into both the mechanism of PVP–PEG complexation and the complex structure.

2. Experimental

PVP (Kollidon K-90), $M_w = 1,000,000$ g mol^{-1}, and PEG ranging in molecular weight from 200 to 36,000 g mol^{-1}, were obtained, respectively, from BASF and Fluka. Dimethyl ether of PEG-400, DMPEG, was purchased from Sigma. All polymers were used as received.

The complete details of the basic experimental procedures employed in this work were introduced in our recent paper [9]. The PVP blends with PEG, covering a full range of compositions, were prepared by dissolving both polymers in a common solvent (ethyl alcohol) followed by removing the solvent by drying at ambient temperature and relative humidity (RH) until weight loss was terminated. Removal of ethyl alcohol from freshly prepared blends was ascertained by FTIR spectroscopy by the absence of methylene group stretching vibrations at 2974 and 1378 cm^{-1} using a Bruker IFS-113v spectrometer with a resolution of 1 cm^{-1} after averaging from 128 scans. The freshly prepared blends and unblended PVP were stored at ambient temperature by equilibrating to controlled pressure of water vapour in desiccators, maintaining RH = 50% at 25°C over different time.

Table 1
Melting temperatures, T_m, and fusion enthalpies, ΔH_m, of PEG employed in this work

Polymer	T_m (°C)	ΔH_m (J g^{-1})
PEG-400	5.9	122.1
PEG-600	15.8	98.3
PEG-1000	39.0	137.4
PEG-36,000	69.1	191.8
DMPEG-400	1.9	106.4

In the d.s.c. apparatus the samples were first quench cooled with liquid nitrogen from ambient temperature to −100°C over 2–3 min and then heated up at a rate of 20°C min^{-1} to 220°C. Upon heating, a heat capacity jump followed by single exotherm coupled with symmetric endotherm, and high temperature endotherm were normally observed for the PVP–PEG blends. These four transitions were, respectively, attributed to the glass transition, PEG cold crystallization, melting, and water thermodesorption [9]. The T_gs were recorded at half-height of the relevant heat capacity jumps in d.s.c. heating thermograms with a Mettler TA 4000/DSC 30 thermoanalyser, calibrated with indium and gallium. The heats of PEG melting peaks were computed by constructing linear baselines from the peak onset to completion and numerically integrated with the appropriate software supplied by Mettler. All reported values are the averages of replicate experiments varying less than 1–2%. Samples of 5–15 mg in weight were sealed in standard aluminium pans supplied with pierced lids so that absorbed the moisture could evaporate upon heating. An argon purge (50 ml min^{-1}) was used to avoid moisture condensation at the sensor. The T_g values for PVP and PEG employed in this research have been presented in Table 1 of the first paper in this series [6].

The weight fractions of crystalline PEG in the blends with amorphous PVP, w_{crPEG}, have been calculated as the ratios of appropriate heats of melting, ΔH_m, of blended PEG to the reference values for unblended PEG, taking into account the weight fraction of absorbed water, w_{H_2O} :

$$w_{crPEG} = \frac{\Delta H_m(\text{blend})}{\Delta H_{mPEG}(1 - w_{H_2O})}. \quad (1)$$

The ΔH_m reference values of unblended crystalline PEG varying in molecular weight, as well as that of DMPEG,

are presented in Table 1. PEG-200 and PEG-300 have not developed any crystallinity during the thermal cycle employed.

The content of absorbed water in the blends was determined by weighing the samples before and after the d.s.c. scans using a Mettler Analytical Balance, AE 240, with an accuracy of ±0.01 mg. Weight loss of the sample after scanning was compared to the amount of desorbed water evaluated from the enthalpy change associated with water evaporation from the sample by d.s.c. Depending on the relative humidity of the surrounding atmosphere, PVP hydration ranged from 6 to 8 wt.%, while PEG contained less sorbed water (0–1 wt.%).

Wide angle X-ray diffraction measurements (WAXS) were performed with filtered Cu Kα radiation using a DRON-3M diffractometer with an asymmetric focusing curved quartz crystal monochromator of a primary beam, equipped with a thermocontrolled cooling camera at −30(±1)°C. Diffraction patterns were recorded in transmission mode. The scattering intensity distribution was measured with a step-scanning device at the step interval of 0.05°, each at the fixed time of 10 s, within the range of twice the Bragg angles from 5 to 50°. Film samples of unblended PVP and PVP–PEG blends over a wide composition range were placed between two PET slides of 0.004 mm in thickness by casting appropriate solutions in ethyl alcohol followed by their drying at ambient temperature. The thickness of the samples was about 1 mm. Similarly, the hermetic PET cells filled with PEG were also used for liquid specimens. In the cooling camera the samples were cooled with liquid nitrogen at a rate of 1°C min^{-1}.

3. Results and discussion

3.1. PEG chain length effects on the negative T_g deviations from the weight-average values

As is shown in the first paper of this series [6], the value of negative deviations from the weight-averaged T_g, w^*_{pl}, describes in fact the number of reactive groups in plasticizer molecules, capable of forming two or three hydrogen bonds with PVP repeat units through the second and third hydroxyl groups. Because all PEG have two proton-donating hydroxyl groups at chain ends, w^*_{PEG} defined by a modified Fox equation (2) in Ref. [6] is expected to be independent of the PEG molecular weight. On the other hand, the concentration of terminal hydroxyl groups in PEG decreases with the increase in molecular weight. From this line of reasoning, only fine or negligible molecular weight effects on the w^*_{PEG} values might be anticipated.

Actually, the obtained w^*_{PEG} values are similar for all PEGs ranging in molecular weight from 200 to 600 g mol^{-1} and follow the pattern shown in Fig. 3 [6] for PEG-400, varying inversely with the PEG weight fraction in the blend, w_{PEG}, and approaching zero in the concentration

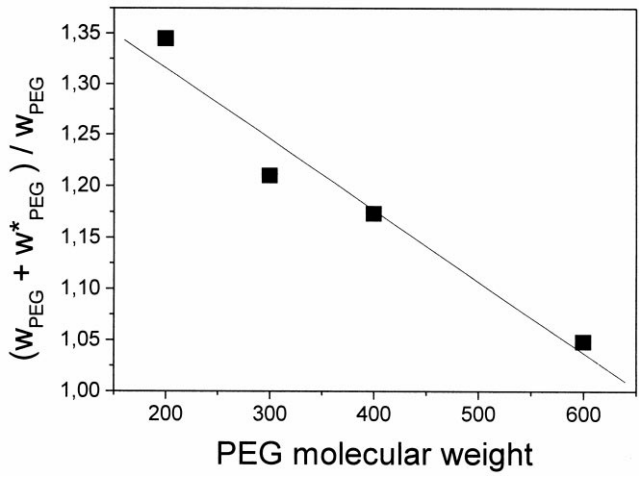

Fig. 1. The involvement of PEG hydroxyl groups into hydrogen bonding with PVP repeat units as a function of PEG molecular weight at [OH]:[PVP] = 1.132.

interval between $w_{PEG} = 0.8$ and 0.9. The latter finding implies that a gradual swelling of the crosslinked PVP–PEG complex in an excess of PEG [6] results in a disruption of the hydrogen-bonded network and the PVP-chains release only in a relatively dilute PVP solution in PEG (10–20%). In other words, the range of PEG concentrations $w_{PEG} = 0.8$–0.9 outlines the border between a swollen PVP–PEG hydrogen-bonded gel and dilute PVP solution in liquid PEG. This conclusion has been supported by the results of independent measurements. As has been recently shown [12], the activation energy for interdiffusion under PVP dissolution in liquid PEG-400 reveals a rapid drop with the increase in PEG concentration within the same region, as is expected for the gel–solution transition.

3.2. The influence of PEG chain length on the degree of hydrogen bonding

The $(w_{PEG} + w^*_{PEG})/w_{PEG}$ ratio describes the involvement of hydroxyl groups at the PEG chain ends in hydrogen bonding to PVP units ([3, Eq. (6)]). With the decrease in PEG concentration the fraction of hydrogen bonded OH groups in PEG molecules increases tending to 2 at zero PEG content. This behaviour is shown for PEG-400 in Fig. 5 in the first paper of this series [6]. Within the PEG-overloaded region, where [OH]/[PVP] > 1, the number of hydrogen-bonded OH groups in the PEG molecule is only slightly influenced by blend composition, considerably exceeding unity but tending to this limit at an enormous PEG excess. Since flexible PEG macromolecules forming two hydrogen bonds with PVP units through both terminal hydroxyls act as a crosslinker, connecting the PVP chains into the supramolecular network structure, this finding indicates the stability of the PVP–PEG network in comparatively dilute PVP solutions in PEG.

Although all PEG chains bear two reactive hydroxyl

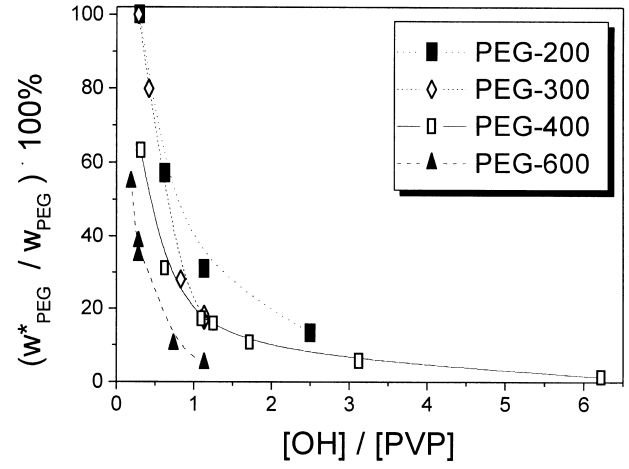

Fig. 2. The plot of the percentage of PEG macromolecules crosslinking PVP units against the number of OH groups available in the blends per one PVP carbonyl.

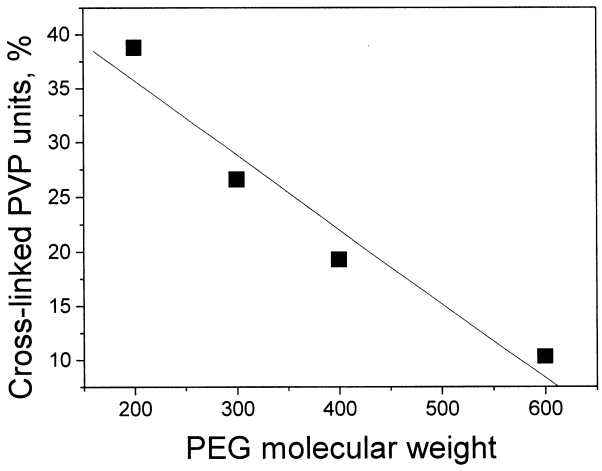

Fig. 4. The content of PVP units (in mole percent) crosslinked by PEG chains in the blend [OH]:[PVP] = 1.132, plotted against the PEG molecular weight.

groups, their hydrogen-bonding activity, expressed in terms of $(w_{PEG} + w^*_{PEG})/w_{PEG}$ ratio, is inversely related to the chain length at a fixed concentration of OH groups in the blend (Fig. 1). As the molecular weight increases approaching 1000 g mol^{-1}, PEG ceases crosslinking PVP units. This conclusion has been confirmed experimentally. The d.s.c. traces of PVP blends with PEG-1000 have been shown to exhibit two glass transitions, which relate to PVP and PEG, respectively. This indicates the incompatibility of PVP with PEG-1000 at a molecular level [3].

3.3. PEG molecular weight as a factor controlling the stoichiometry of the hydrogen-bonded PVP–PEG network

The ratio w^*_{PEG}/w_{PEG} defines the weight fraction of PEG macromolecules crosslinking PVP chains by hydrogen bonding through both terminal hydroxyls. The crosslinking capability of PEG chains increases with the decrease in their length as well as with the reduction in the number of PEG hydroxyls available in blends per one PVP unit (Fig. 2). Using the w^*_{PEG}/w_{PEG} ratio, the dynamics of hydrogen bonding and crosslinking capability of the PVP units has been described in terms of the quantities outlined by Eqs. (4) and (5) presented in the first paper of this series [6]. Comparison of the number of hydrogen-bonded PVP repeat units for PVP blends with PEG-200, -300 and -600 with that for PEG-400, displayed in Fig. 7 in Ref. [6], highlights the influence of PEG chain length on the state of PVP carbonyls. Qualitatively, the dynamics of PVP hydrogen bonding with PEG-200, -300 and -600 follows the pattern shown by PEG-400 [6, Fig. 7], however the quantitative distinctions are evident, particularly in the percentage of PVP units crosslinked through telechelic PEG chains. To make the comparison more readily illustrative, the concentration profiles of the amount of PVP units, crosslinked through PEG chains varying in molecular weight from 200 to 600, are presented in Fig. 3.

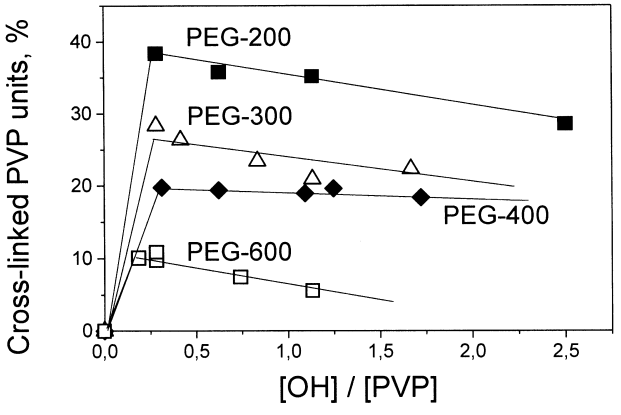

Fig. 3. Impact of PEG molecular weight upon the compositional behaviour of the percentage of PVP units crosslinked through PEG chains.

The content of crosslinked PVP units is nearly independent of PEG concentration over a wide composition range for a variety of PEGs ranged in molecular weight, indicating the stoichiometry of hydrogen-bonded network PVP–PEG complexes. The most stable, toward swelling with an excess of PEG, is the PVP complex with PEG-400, while other PEGs reveal a noticeable reduction in the content of crosslinked PVP units with the increase in PEG concentration. The crosslinking degree of PVP units in the stoichiometric complexes, shown in Fig. 4 as a function of PEG molecular weight, follows the pattern demonstrated in Fig. 1 for the hydrogen-bonding reactivity of PEG. Both the involvement of PEG chain-end hydroxyls into hydrogen bonding with PVP (Fig. 1) and the amount of crosslinked PVP units in the stoichiometric complex (Fig. 4) are found to relate inversely to the PEG molecular weight, allowing us to gain an insight into the structure of the stoichiometric supramolecular PVP–PEG network complex.

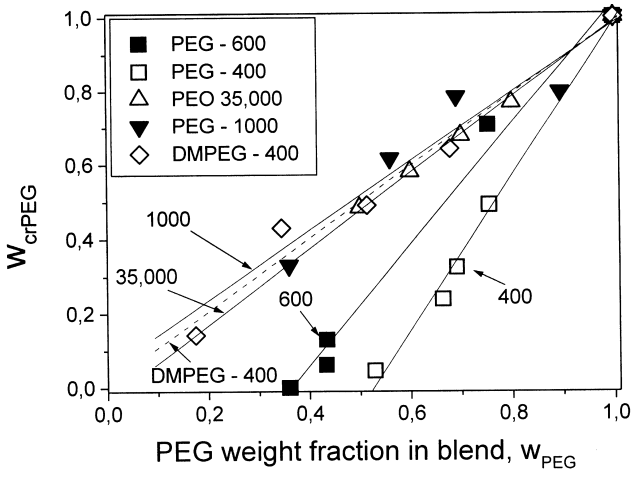

Fig. 5. The weight fraction of crystalline PEG, w_{crPEG}, in blends with amorphous PVP as a function of PEG weight fraction, w_{PEG}, for the PEG varied in molecular weight from 400 to 36,000 g mol^{-1} and for dimethyl ether of PEG-400, DMPEG.

The stoichiometric composition of the PVP complex with PEG-400, established via the analysis of the compositional behaviour of w^*_{PEG}, has been earlier shown to be in reasonable agreement with the data of independent measurements, such as FTIR spectroscopy and the relation of the amount of noncrystallizing PEG-400 to blend composition, determined from d.s.c. heating thermograms [5,6]. In order to give additional credit to the w^*_{PEG}-based approach for describing correctly the stoichiometry of the PVP–PEG complex, the composition dependence of PEG crystallinity in the blends with amorphous PVP is considered in Fig. 5. PEG-200 and PEG-300 have been found to develop no crystallinity during the quench-cooling/heating cycle employed in this research for d.s.c. measurements.

In Fig. 5 the weight fractions of crystalline PEG, w_{crPEG}, are plotted against total PEG content, w_{PEG}. If amorphous PVP merely diluted crystalline PEG and did not interfere with its crystallinity through a strong favourable interaction such as hydrogen bonding, the plot would represent a straight line connecting the origin and the crystallinity degree of pure PEG, defined as $w_{crPEG} = 1$. This ideal dilution behaviour is in fact typical of the PVP blends with those PEGs which provide no or negligible contribution of end-chain hydroxyls (DMPEG-400 and comparatively long-chain PEG having molecular weights of 1000 g mol^{-1} and higher). In contrast, the disappearance of melting peaks in the d.s.c. scans due to free PEG-400 and PEG-600 within the PVP-overloaded blends, and the lack of equivalence between the crystallinity (w_{crPEG}) and the total amount of PEG in the PEG-overloaded systems, are the proofs for PEG being hydrogen bonded with PVP in the blends enriched by amorphous PVP. This has been shown earlier analysing in detail both kinetic and thermodynamic contributions to the depression of PEG-400 crystallinity in the blends with PVP [7].

The data in Fig. 5 provide a feasible method of estimating the amount of bound (noncrystallizing) PEG from the appropriate intercepts at $w_{crPEG} = 0$. The binding degree obtained in this manner is found to be $w_{PEG} \approx 0.526$ for PEG-400 and ~0.364 (g PEG/g blend) for PEG-600 (Fig. 5). The obtained values correspond to ~0.308 and ~0.106 bound macromolecules of PEG-400 and PEG-600 per one PVP repeat unit available in the blends. Accordingly, in total ~61.6 and 23.2% of PVP repeat units have been hydrogen bonded to terminal hydroxyls in the complexes with PEG-400 and PEG-600, respectively. In full agreement with the data in Fig. 4, determined by the analysis of the behaviour of w^*_{PEG} vs. composition, the binding degrees of PEG-400 and PEG-600, found from the intercepts in Fig. 5, relate to each other as the reciprocals of their molecular weights:

$$\frac{w_{PEG\text{-}600}(w_{crPEG} = 0)}{w_{PEG\text{-}400}(w_{crPEG} = 0)} = \frac{0.364}{0.526} = 0.69 \approx \frac{MW_{PEG\text{-}400}}{MW_{PEG\text{-}600}} = \frac{400}{600} = 0.67. \quad (2)$$

From the T_g–composition relationship, the total amount of crosslinked PVP units and that hydrogen bonded to the PEG macromolecules, having one of the ends free of hydrogen bonding with PVP, can be obtained as the sum of M_1 and M_2 quantities, defined by Eqs. (4) and (5) in Ref. [6]. At the PEG concentration ([OH]:[PVP] ≈ 0.30) corresponding to the onset of the limiting values of the content of PVP units crosslinked by PEG-400 (~20%) and PEG-600 (~10%), we get $M_1 + M_2 \approx 62\%$ for PVP bonding to PEG-400 [6, Fig. 7] and $M_1 + M_2 \approx 20\%$ for PEG-600. The values found match closely to that obtained from blend crystallinity. Consequently, the analysis of blend crystallinity allows estimating the total amount of bound PEG, but provides no distinctions between strongly (crosslinked) and loosely bound PEG. The varieties of bound PEG may be however determined with both the w^*_{PEG}-based approach and FTIR spectroscopy.

The linearity of the plots for PEG-400 and PEG-600 crystallinity in Fig. 5 reveals the invariability of the appropriate intercepts over PEG-overloaded composition range, i.e. the stoichiometry of PVP hydrogen-bonded complexes with PEG-400 and PEG-600. At an excess of PEG, only w^*_{PEG}-analysis provides an unambiguous measure of the amount of crosslinked PVP units, defined earlier as strongly bound [6]. At the same time, the FTIR data for PVP blends with PEG-400, presented in Table 2 of the first paper in this series [6], demonstrate that even in comparatively dilute (15%) PVP solution in liquid PEG-400 (at [OH]:[PVP] = 2.8) both the total amount of hydrogen-bonded PVP units (56 mol%) and that strongly bound (26.2%) remain nearly invariant with changing composition. Thus, the analysis of PEG fusion enthalpy and FTIR spectroscopy confirm the applicability of the w^*_{PEG}-based approach for describing the stoichiometry of PVP–PEG hydrogen-bonded complexes using the T_g–composition relationship. In a subsequent section of this

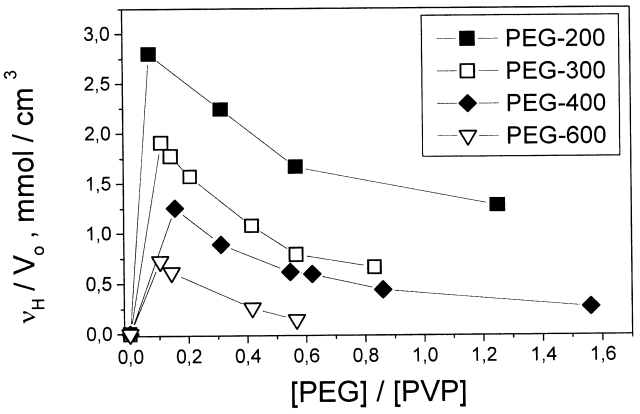

Fig. 6. The plot of hydrogen-bonded crosslink density, ν_H/V_0, against the composition of PVP blends with PEG varied in molecular weight from 200 to 600 g mol^{-1}.

paper we will present the WAXS data supporting the data shown in Fig. 5 for the crystallinity of PVP blends with PEG-400 and PEG-600.

3.4. Influence of PEG chain length on network density in hydrogen-bonded stoichiometric PVP–PEG complexes

Mixing glassy PVP with short chain PEG is a two-stage process [13]. At the first stage, when comparatively a small amount of plasticizer is added to PVP, the T_g falls dramatically over 220°C. This stage may be treated as PVP plasticization due to hydrogen bonding of carbonyls to PEG terminal hydroxyls. Since the hydroxyls are located at the PEG chain ends, and because within PVP-overloaded blends both PEG terminal hydroxyls are found to be involved in hydrogen bonding by crosslinking PVP units (Fig. 3), the relatively short PEG chains serve as spacers, creating free volumes between longer PVP chains [3]. The fraction of free volume may be evaluated from the blends' T_g using a combination of the Doolittle and Williams–Landell–Ferry (WLF) equations [14].

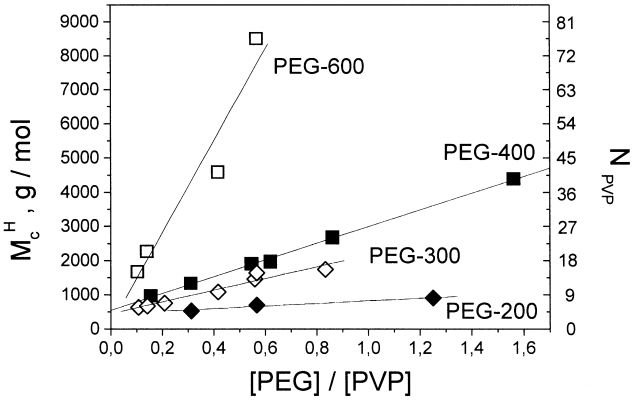

Fig. 7. The average molecular weight (M_c^+) of the PVP chain segment between neighbouring hydrogen-bonded PEG crosslinks, and the average number of polymer repeat units in this segment, N_{PVP}, in the course of PVP–PEG network complex swelling in excess PEG.

The second stage of the PVP–PEG mixing process reveals comparatively insignificant T_g reduction, that is indicative of weaker PVP–PEG interaction. This stage has been defined as a gradual swelling and dissolution of the PVP–PEG crosslinked complex in an excess of PEG [13]. The boundary between the first and second stages corresponds to the stoichiometric composition of the PVP–PEG complex.

Based on these arguments, one could expect that the longer the chains of the PEG crosslinker, serving as a spacer between the PVP and PEG chains in the network complex, the larger the free volume, i.e. the greater the T_gs decrease under PVP–PEG mixing. However, this is not the case for PVP blends with different PEG where the effect of PEG molecular weight on the blends' T_g has been found to be comparatively insignificant. The fractional free volume in PVP blends with PEGs, ranging in molecular weight from 200 to 600 g mol^{-1}, is nearly unaffected by the PEG chain length. The reason for this behaviour is the compensating effect of the PEG chain length on the density of hydrogen-bonded crosslinks in the PVP–PEG network.

Knowing w^*_{PEG} and applying Eq. (6), presented in the first paper of this series [6], make feasible estimating the density of hydrogen-bonded entanglements, ν_H/V_0, in the PVP–PEG network (Fig. 6). The average critical molecular weight of the PVP chain segment between neighbouring junctions of the hydrogen-bonded network, M_c^+, may be evaluated using a simple relation:

$$\frac{\nu_H}{V_0} = \frac{\rho}{M_c^+} \tag{3}$$

where ρ is a blend density. The M_c^+ behaviour is illustrated in Fig. 7 along with an average number of PVP repeat units in the chain segment between hydrogen-bonded junctions, N_{PVP}. The shorter the chains of the PEG crosslinker the larger the density of the network. The maximum of the PVP–PEG network density (Fig. 6) corresponds to the onset of the steady-state content of the crosslinked PVP units (Fig. 3), which in turn relates to the minimum PEG concentration providing the formation of a stoichiometric complex. In full agreement with the two-stage model of the PVP–PEG mixing mechanism, subsequent addition of PEG results in a gradual decrease of the PVP–PEG network density (Fig. 6), which is typical for swelling gels. Both the M_c^+ and N_{PVP} quantities are the linear functions of the blend composition (Fig. 7). The longer the PEG chain the easier the network swells in an excess of PEG, i.e. the longer the PVP chain segment between neighbouring crosslinks. The PVP–PEG-200 network swelling is accompanied by relatively slight growth in the length of the PVP chain segment between neighbouring hydrogen-bonded network junctions, compared to PEG of higher molecular weight. The swelling of the PVP complex with PEG-200 results, however, in a significant reduction of network density (Fig. 6). This is a direct consequence of the rise in PVP

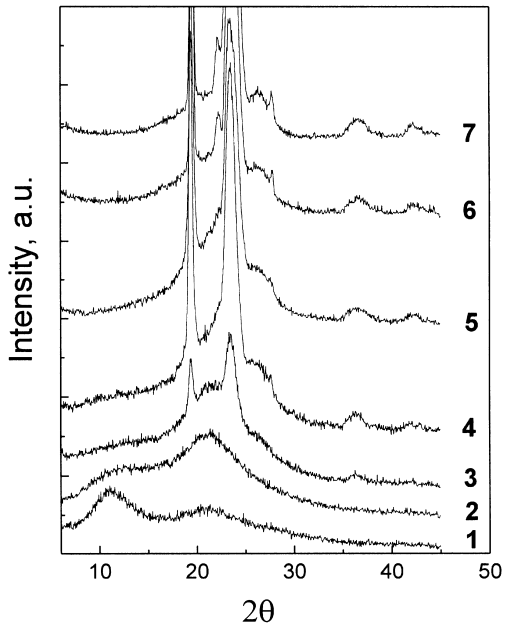

Fig. 8. X-ray diffraction patterns of PVP, PEG-400, and their blends over entire composition range at −30°C: (1) 100% PVP; (2) 36% PEG; (3) 53% PEG; (4) 69% PEG; (5) 85% PEG; (6) 92% PEG; (7) 100% PEG.

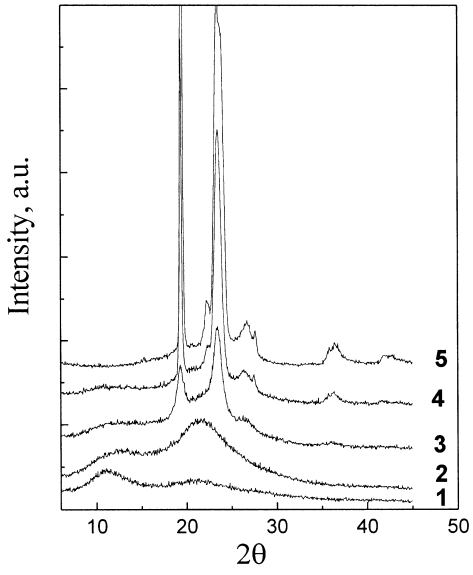

Fig. 9. X-ray diffraction patterns of PVP, PEG-600, and their blends over a wide composition range at −30°C: (1) 100% PVP; (2) 36% PEG; (3) 53% PEG; (4) 69% PEG; (5) 100% PEG.

crosslinking degree as the length of the PEG chain decreases (Figs. 3 and 4).

The effects of PEG chain length on the parameters of the hydrogen-bonded network, displayed in Figs. 6 and 7, are analysed by including the molecular weight terms into Eq. (6) [6], employed for evaluation of ν_H/V_0, M_c^+ and N_{PVP} using w^*_{PEG}. Therefore, it would of great importance to compare the established PEG chain length effects to the data of independent measurements. Figs. 8 and 9 demonstrate the contributions of PEG molecular weight to the structure of PVP solutions in PEG-400 and PEG-600 revealed by X-ray diffraction patterns.

The X-ray diffraction pattern of unblended PVP shows two broad peaks at 11.3 and 21.3°, which correspond to a period of ~0.718 and ~0.417 nm, respectively [15]. According to Killian and Boueke [16], the first halo of the amorphous polymer is most likely due to interchain interference, while the second one corresponds to the scattering from side chains. Hence, the first peak characterizes the periodicity of PVP backbones arrangement, whereas the second halo relates to the scattering from pyrrolidone rings in PVP side chains. The X-ray scattering curves of PEG-400 and PEG-600 at −30°C exhibit two sharp peaks of crystalline polymer at 19.3 and 23.4°. Dilution of crystalline PEG with amorphous PVP results in the depression of PEG crystallization. No crystalline phase occurs in the blends containing up to 50 wt.% of PEG-400 and 36 wt.% of PEG-600, which is in excellent agreement with the data of d.s.c. measurements presented in Fig. 5. Note, that PEG-600 crystallization begins at lower concentration compared to PEG-400 behaviour. This finding has been assigned to the higher binding degree of PEG-400 in the stoichiometric complex with amorphous PVP (Fig. 3). The PVP–PEG blending also leads to a rapid decrease in the intensity of the halo at 11.3°, which is an evidence for the loss of contacts between the repeat units of the neighbouring PVP chains. In the blend containing 36 wt.% of PEG, where the stoichiometric complex is just formed, the PVP interchain contacts are still manifested by a shoulder on the scattering curves around 11.3°. Subsequent swelling of the PVP–PEG network in an excess of PEG causes the decrease in PVP interchain contacts at ~50 wt.% of PEG-400, whereas these are still observed in the blends containing 69 wt.% of PEG-600. This is an unambiguous

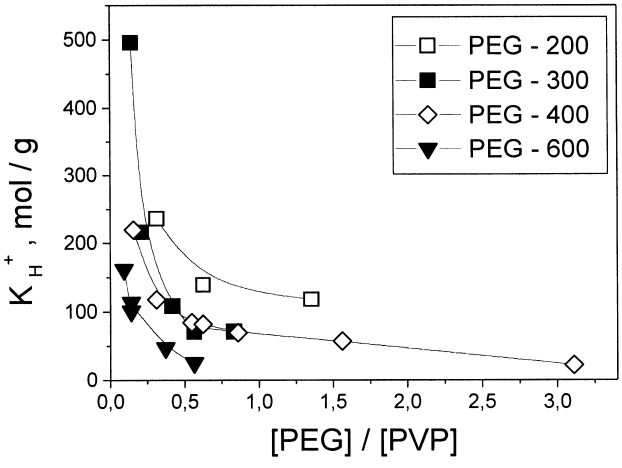

Fig. 10. The composition dependence of the constant of PVP hydrogen-bonded crosslinked stoichiometric complex formation, K_H^+ (mol g^{-1}), with PEG varied in molecular weight from 200 to 600 g mol^{-1}.

consequence of a sparse PVP–PEG-600 hydrogen bonded network. The contribution of PEG spacer length to the suppression of PVP interchain contacts within the network complex is thought to be negligible compared to that of the length of the PVP chain segment between neighbouring hydrogen-bonded network junctions, controlled by crosslinking degree. Actually, the PEG chains are highly flexible. The PEG chain segment has been reported to consist of 4–5 monomer units [17]. This is twice as low as the total number of oxyethylene units in the PEG-400 chain, and trice as that in the PEG-600 chain. Thus, the results for the PVP–PEG network density, obtained from w^*_{PEG}, are consistent with the structure of the PVP–PEG hydrogen-bonded complex established with the WAXS technique.

3.5. Equilibrium constants and energy of PVP–PEG association into hydrogen-bonded crosslinked stoichiometric complex

Like an individual chemical compound, the stoichiometric PVP–PEG complex demonstrates a composition independent of the concentration of the parent components in the blend. This is the case not only at the stage of crosslinked complex swelling and dissolution in an excess of PEG as is evident from the data in Fig. 3, but within the entire composition range. The PVP-overloaded blends ($w_{PEG} < 0.36$) have been found to separate into the stoichiometric PVP complex and the parent PVP, as is indicated by the occurrence of two T_gs around -30 and 50°C, which correspond to the complex and hydrated PVP, respectively [5]. With the rise of PEG concentration up to 36 wt.%, the change in heat capacity between the rubbery and glassy state, ΔC_p, accounted for the first transition grows, whereas the latter decreases. For the blends with $w_{PEG} > 0.36$ only lower temperature glass transition is observed from d.s.c. traces. Consequently, the process of hydrogen-bonded crosslinked PVP–PEG complex formation may be treated as a chemical equilibrium, described by the constant K^+_H (mol g^{-1}), which can be expressed in terms of w^*_{PEG} and w_{PEG}:

$$K^+_H = \frac{2w^*_{PEG}}{(2w_{PEG} - w^*_{PEG})\left(\frac{w_{PVP}}{MW_{PVP}} - \frac{2w^*_{PEG}}{MW_{PEG}}\right)} \quad (4)$$

where MW_{PVP} is the molecular weight of the PVP repeat unit (111.14 g mol^{-1}) and MW_{PEG} is the molecular weight of the PEG macromolecule (200, 300, 400 and 600 g mol^{-1}).

In accordance with Le Châtelier's principle, a small change in composition, such as that caused by the addition or removal of one of the reactants or the product, shifts the position of the equilibrium accordingly. Consequently, K^+_H varies with blend composition, as is illustrated in Fig. 10. K^+_H is a measure of the tendency of the complexation to occur. If it is a large and positive number, the concentration of the PVP–PEG complex at equilibrium is large compared to those of active reactants, [OH] and [PVP]. This is the case for the blends containing an excess of PVP, i.e. at the stage of PVP–PEG complex formation, whereas at the stage of the complex swelling and dissolution in an excess of PEG, K^+_H drops significantly tending to zero at considerable PEG overloading. The effect of PEG molecular weight on K^+_H is, the shorter PEG chain the stronger the association (Fig. 10).

The equilibrium constant of the PVP–PEG stoichiometric complex formation provides a bridge to the standard free energy change for PVP–PEG association into hydrogen-bonded crosslinked stoichiometric complex, ΔG^+_H. The latter relates to the equilibrium constant through the fundamental van't Hoff equation:

$$\Delta G^+_H = -RT \ln K^+_H. \quad (5)$$

The compositional profiles of the free energy for PVP curing by hydrogen bonding through short PEG chains are presented in Fig. 11. Large K^+_H values correspond to the large negative ΔG^+_H magnitudes. The PVP–PEG complex formation is an exothermic process and the gain in energy is greater at the first stage of PVP plasticization due to hydrogen bonding with PEG ([PEG]:[PVP] < 0.5 or [OH]:[PVP] < 1), than at the second stage of PVP–PEG complex swelling and dissolution in an excess of PEG. The shorter the PEG chain the larger the gain in energy under PVP–PEG complex formation. This fundamental conclusion leads to understanding the reason for nonequimolar stoichiometry of PVP–PEG hydrogen bonding.

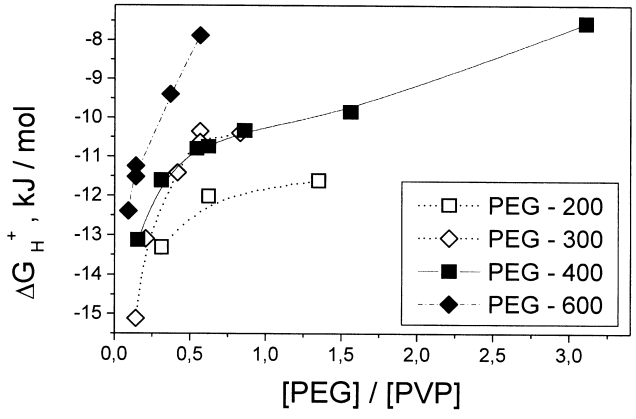

Fig. 11. Effects of blend composition and PEG molecular weight on the standard free energy change (ΔG^+_H, kJ/mol^{-1}) for hydrogen-bonded stoichiometric network PVP–PEG complex formation at 20°C.

3.6. Molecular structure of stoichiometric complex and PVP–PEG hydrogen-bonding thermodynamics

Every PEG macromolecule bears only two hydroxyl reactive groups at opposite chain ends. The energy of "strong" PVP hydrogen-bonds with PEG-400, measured from FTIR spectra, has been found to be 21.42 kJ mol^{-1} [4], whereas the data in Fig. 11 give the values of the order of 10–13 kJ mol^{-1} and show the ΔG^+_H variation with composition. This apparent

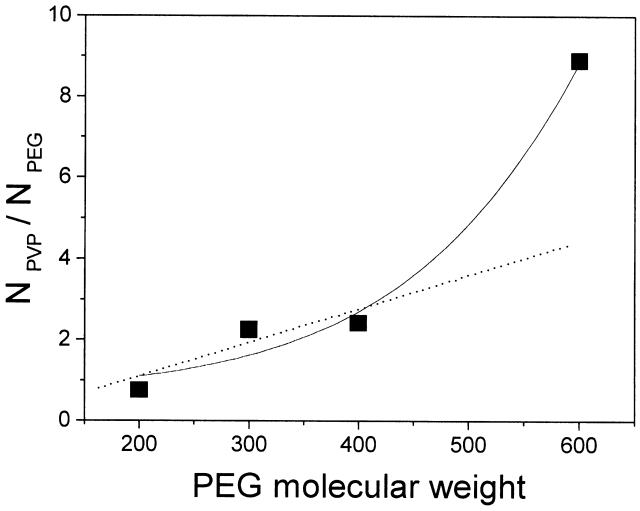

Fig. 12. The number of PVP repeat units per one PEG monomer unit in the mesh between neighbouring hydrogen-bonded crosslinks plotted against the PEG molecular weight. The N_{PVP}/N_{PEG} ratio is evaluated from appropriate slopes of linear plots in Fig. 7.

discrepancy is explicable, because the total free energy of mixing has been embedded in a specified T_g value, which includes both enthalpy and entropy contributions [18], as well as that due to PEG self-association [19]. At the same time, the FTIR data characterize rather an enthalpy of a single hydrogen bond. In our particular case, by the definition of the PVP–PEG complex formation equilibrium constant, outlined by Eq. (4), ΔG_H^+ represents only a constituting part of the total free energy of mixing, which accounts for PVP hydrogen-bond crosslinking with PEG. Compared to the magnitude obtained from the FTIR data, ΔG_H^+ appears to be smaller due to a negative change in entropy under PVP–PEG hydrogen-bonded association into a supramolecular network structure.

Hydrogen bonding of PEG terminal hydroxyls to the carbonyls in PVP repeat units causes inevitable loss in entropy due to the decrease in the number of degrees of freedom of the PEG chains attached to longer PVP macromolecules through two hydrogen bonds at both PEG chain ends. Unblended PVP is in a glassy state and its segmental mobility is essentially frozen. The PVP plasticization (due to hydrogen bonding with PEG) results in the growth of mobility since the lower the T_g the larger the free volume and higher the mobility. Within the PEG-underloaded region ([PEG]:[PVP] < 0.5) the loss in entropy due to PEG chains immobilization can be still counterbalanced by the increase in the mobility of PVP chain segments between neighbouring cross-links, caused by free volume formation under PVP–PEG hydrogen bonding. It means that PVP curing by PEG short chains is thermodynamically allowed only if the length of the PVP chain segments between neighbouring hydrogen-bonded network junctions is above some critical value which depends on the length of the crosslinking PEG chains. The longer the PEG chains the larger the loss in entropy due to their immobilization and greater must be the counterbalancing increase in PVP segmental mobility. The latter requires a longer PVP chain segment between neighbouring crosslinks, i.e. a sparser hydrogen-bonded PVP–PEG network and, consequently, the lower crosslinking degree of PVP units in the hydrogen-bonded stoichiometric complex. As PVP chains have already obtained sufficient mobility in the flexible network of the PVP–PEG complex, they become unable to compensate the further loss in PEG chain entropy during the course of hydrogen bonding. For this reason the PEG macromolecules cease to form hydrogen bonds with PVP units through the second terminal hydroxyl groups, and the crosslinked complex has achieved its stoichiometric composition. All these phenomena have been in fact observed in PVP–PEG systems as is shown in this study.

Although the length of the PVP segment between neighbouring junctions of the hydrogen-bonded network is mainly determined by the length of crosslinking PEG chain, the ratio between these lengths is supposed to develop some degree of misbalance with the increase in PEG molecular weight due to growing contribution of van der Waals interactions between neighbouring PEG chains in the hydrogen-bonded network. If merely the entropic contribution had governed the frequency of PEG hydrogen-bonded crosslinks, the N_{PVP}/N_{PEG} ratio would be independent on PEG chain length. However, as Fig. 12 demonstrates, the ratio of the length of the PVP-segment between neighbouring junctions to that of PEG chain increases monotonously with PEG molecular weight within the range from 200 to 400 g mol^{-1}. At the same time, comparatively longer PEG spacers, exemplified by PEG-600, reveal significantly sparser networks, i.e. the PVP chain segment between neighbouring crosslinks becomes longer. The nonlinear character of the relationship in Fig. 12, coupled with the linearity of the dependence of the PVP crosslinking-degree on the PEG molecular weight (Fig. 4) is indicative of an enthalpy contribution to the process of PEG chains distribution within the crosslinked stoichiometric complex. Indeed, the longer the PEG chains and greater the contribution of the PEG interchain interactions, the stronger is the trend of PEG assembling into hydrogen bonding clusters of extended chains within the PVP–PEG network. Hydrogen bonding of PVP with PEG cannot interfere with PEG clusterization. By this means, comparatively shorter PEG chains hydrogen bonded to PVP units through terminal hydroxyl groups appear to be more or less uniformly distributed along PVP chains. In contrast, longer PEG chains exhibit a tendency of association. As a result, the PVP macromolecules are crosslinked by the clusters of extended PEG chains. Such clusters resemble PEG crystallites, where terminal hydroxyl groups are exposed outward crystalline grains. At this instance, the molecular structure of the PVP–PEG stoichiometric complex can be treated as PVP chains adsorbed on the end faces of PEG crystallites through hydrogen bonding of the PVP units to the PEG end-chain hydroxyls. This

conjecture has been in fact supported by our finding that PEG blends with a small amount of PVP demonstrate significantly higher melting temperature than that found for unblended PEG [20].

4. Conclusions

The observed relation of the negative T_g deviations from the weight-average values to the weight fraction of PEG macromolecules, which form with PVP repeat units two hydrogen bonds, provides a convenient tool to evaluate the stoichiometry of the PVP–PEG hydrogen-bonded complexes, their crosslinking degree and energy of formation, as well as the density and molecular structure of the hydrogen-bonded network. The analysis of PEG chain length effects on a variety of PVP–PEG hydrogen-bonding characteristics allows obtaining an insight into the thermodynamics of polymer interaction over the entire composition range. The nonequimolar stoichiometry of PVP–PEG hydrogen-bonded network complexes is a result of specific balance between the *loss in entropy* due to the *immobilization of short PEG chains* in the course of their hydrogen bonding to PVP units through both chain ends, and the *entropic gain* due to the *increase in mobility of PVP-chain segments* between neighbouring hydrogen-bonded junctions in the network. The competition between these two factors eventually determines the observed increase in the PVP crosslinking degree with the decrease in PEG molecular weight and defines the nonequimolar stoichiometry of the formed hydrogen-bonded complexes.

Acknowledgements

This research was in part made possible by Award No. RC1-2057 of the US Civilian Research & Development Foundation for the Independent States of the Former Soviet Union (CRDF). We express our appreciation to Professors Alexander Yu. Grosberg, Ronald A. Siegel, Anatoly E. Chalykh, and Dr Elena Dormidontova for their helpful discussion and comments.

References

[1] Cesteros LC, Quintana JR, Fernandez JA, Katime I. Miscibility of poly(ethylene oxide) with poly(N-vinyl pyrrolidone): DMTA and DTA studies. J Polym Sci, Polym Phys Ed 1989;27:2567–76.

[2] Buehler V. Kollidon: polyvinylpyrrolidone for the pharmaceutical industry. 3rd ed. Ludwigshafen: BASF, 1996 (p. 19–20).

[3] Feldstein MM, Lebedeva TL, Shandryuk GA, Kotomin SV, Kuptsov SA, Igonin VE, Grokhovskaya TE, Kulichikhin VG. Complex formation in poly(N-vinyl pyrrolidone–poly(ethylene glycol) blends. Polym Sci 1999;41(8):854–66.

[4] Lebedeva TL, Igonin VE, Feldstein MM, Platé NA. H-bonding poly-(ethylene glycol) to poly(N-vinyl pyrrolidone) within an adhesive hydrogel matrix for transdermal drug delivery. Proc. Int. Symp. Control. Release Bioact. Mater., vol. 24, 1997. p. 447–8.

[5] Feldstein MM, Lebedeva TL, Shandryuk GA, Igonin VE, Avdeev NN, Kulichikhin VG. Stoichiometry of poly(N-vinyl pyrrolidone)–poly(ethylene glycol) complex. Polym Sci 1999;41(8):867–75.

[6] Feldstein MM, Shandryuk GA, Platé NA. Relation of glass transition temperature to the hydrogen bonding degree and energy in poly(N-vinyl pyrrolidone) blends with hydroxyl-containing plasticizers: 1. Effects of the number of hydroxyl groups in plasticizer molecule. Polymer 2001;42(3):971–9.

[7] Feldstein MM, Kuptsov SA, Shandryuk GA. Coherence of thermal transitions in poly(N-vinyl pyrrolidone)–poly(ethylene glycol) compatible blends: 2. The temperature of maximum cold crystallization rate versus glass transition. Polymer 2000;41(14):5339–48.

[8] Feldstein MM, Chalykh AE, Chalykh AA, Platé NA. Quantitative relationship between molecular structure and adhesion of PVP–PEG hydrogels. Polym Mater Sci Engng 1999;81:465–6.

[9] Feldstein MM, Shandryuk GA, Kuptsov SA, Platé NA. Coherence of thermal transitions in poly(N-vinyl pyrrolidone)–poly(ethylene glycol) compatible blends: 1. Interrelations among temperatures of melting, maximum cold crystallization rate and glass transition. Polymer 2000;41(14):5327–38.

[10] Feldstein MM, Bairamov DF. Effects of chain orientation, free volume and interaction on glass transition in poly(N-vinyl pyrrolidone)–poly(ethylene glycol) blends involving a stoichiometric hydrogen-bonded network complex. Polym Mater Sci Engng 2000;82:365–6.

[11] Fox TG. Influence of diluent and copolymer composition on the glass transition temperature of a polymer system. Bull Am Phys Soc 1956;1:123.

[12] Igonin VE, Makarova VV, Avdeev NN, Feldstein MM, Kulichikhin VG. Optical microinterference measurements of polymer miscibility, dissolution and interdiffusion. Proc. Int. Symp. Control. Release Bioactive Mater., vol. 26, 1999. p. 391–2.

[13] Feldstein MM. A two-stage mechanism of poly(N-vinyl pyrrolidone) mixing with short-chain poly(ethylene glycol). Proc. Int. Symp. Control. Release Bioact. Mater., vol. 25, 1998. p. 848–9.

[14] Ferry JD. Viscoelastic properties of polymers. 2nd ed. New York: Wiley, 1970 (chap. 11).

[15] Guinier A. Théorie et technique de la radiochristallographie, 2nd ed. Paris: Dunod, 1956 (chap. 12, paragraph 3).

[16] Killian HG, Boueke K. Röntgenographische Strukturanalyse von amorphem Polystirol. VI. J Polym Sci 1962;58(16):311–33.

[17] Bershtein VA, Egorov VM. Differential scanning calorimetry of polymers. New York: Horwood, 1994 (chap. 1).

[18] Wu J. The glassy state, ideal glass transition, and second-order phase transition. J Appl Polym Sci 1999;71:143–50.

[19] Coleman MM, Graf JF, Painter PC. Specific interactions and the miscibility of polymer blends. Lancaster: Technomic, 1991 (chap. 4).

[20] Feldstein MM, Kuptsov SA, Shandryuk GA, Platé NA, Chalykh AE. Coherence of thermal transitions in poly(N-vinyl pyrrolidone)–poly-(ethylene glycol) compatible blends: 3. Impact of sorbed water upon phase behaviour. Polymer 2000;41(14):5349–59.